CCFE-PR(15)57

K.G. McClements, R.J. Akers, W.U. Boeglin,
M. Cecconello, D. Keeling, O.M. Jones, A. Kirk,
I. Klimek, R.V. Perez, K. Shinohara and K. Tani

The effects of resonant magnetic perturbations on fast ion confinement in the Mega Amp Spherical Tokamak

The effects of resonant magnetic perturbations on fast ion confinement in the Mega Amp Spherical Tokamak

K.G. McClements[1], R.J. Akers[1], W.U. Boeglin[2], M. Cecconello[3], D. Keeling[1], M. Jones[1;4,] A. Kirk[1], I. Klimek[3], R.V. Perez[2], K. Shinohara[5] and K. Tani[6]

[1] CCFE, Culham Science Centre, Abingdon, Oxfordshire, OX14 3DB, UK
[2] Department of Physics, Florida International University, 11200 SW 8th Street, Miami, Florida 33199, USA
[3] Department of Physics and Astronomy, Uppsala University, SE-751 05, Uppsala, Sweden
[4] Department of Physics, Durham University, South Road, Durham DH1 3LE, UK
[5] Japan Atomic Energy Agency, Naka, Ibaraki 311-0193, Japan
[6] Nippon Advanced Technology Co., Ltd, Naka, Ibaraki 311-0102, Japan

The effects of resonant magnetic perturbations on fast ion confinement in the Mega Amp Spherical Tokamak

K.G. McClements[1], R.J. Akers[1], W.U. Boeglin[2], M. Cecconello[3], D. Keeling[1], O.M. Jones[1,4], A. Kirk[1], I. Klimek[3], R.V. Perez[2], K. Shinohara[5] and K. Tani[6]

[1] CCFE, Culham Science Centre, Abingdon, Oxfordshire, OX14 3DB, UK
[2] Department of Physics, Florida International University, 11200 SW 8th Street, Miami, Florida 33199, USA
[3] Department of Physics and Astronomy, Uppsala University, SE-751 05, Uppsala, Sweden
[4] Department of Physics, Durham University, South Road, Durham DH1 3LE, UK
[5] Japan Atomic Energy Agency, Naka, Ibaraki 311-0193, Japan
[6] Nippon Advanced Technology Co., Ltd, Naka, Ibaraki 311-0102, Japan

Abstract

The effects of resonant magnetic perturbations (RMPs) on the confinement of energetic (neutral beam) ions in the Mega Amp Spherical Tokamak (MAST) are assessed experimentally using measurements of neutrons, fusion protons and fast ion Dα (FIDA) light emission. In single null-diverted (SND) MAST pulses with relatively low plasma current (400kA), the total neutron emission dropped by approximately a factor of two when RMPs with toroidal mode number $n = 3$ were applied. The measured neutron rate during RMPs was much lower than that calculated using the TRANSP plasma simulation code, even when non-classical (but axisymmetric) *ad hoc* fast ion transport was taken into account in the latter. Sharp drops in spatially-resolved neutron fluxes, fusion proton fluxes and FIDA emission were also observed. First principles-based simulations of RMP-induced fast ion transport in MAST, using the F3D-OFMC code, show similar losses for two alternative representations of the MAST first wall, with and without full orbit effects taken into account; for $n = 6$ RMPs in a 600kA plasma, the additional loss of beam power due to the RMPs was found in the simulations to be approximately 11%.

1 Introduction

Three-dimensional field perturbations are frequently added (using external coils) to the otherwise axisymmetric equilibrium magnetic fields in tokamak plasmas with the aim of suppressing edge localised modes (ELMs), or at least ameliorating their effects. It has been found in ASDEX Upgrade [1], KSTAR [2] and DIII-D [3] that such fields, often referred to as resonant magnetic perturbartions (RMPs), can degrade the confinement of energetic ions. However there is also evidence that the deconfining effect of a departure from axisymmetry (associated with the fact that toroidal canonical momentum is no

longer a constant of the motion for collisionless particles) is offset in at least some cases by the accompanying reduction in ELM amplitudes, since ELMs themselves can cause fast ion losses [1]. The overall effect of externally-applied field perturbations on fast ion confinement is therefore rather complex, and it is not at all clear how results in existing experiments can be extrapolated to future devices, in particular ITER. There has been some predictive modelling of the effects of RMPs (but not ELMs) on the confinement of fusion alpha-particles and beam ions in ITER, specifically in steady-state scenarios with plasma current $I_p = 9\,\mathrm{MA}$ [4, 5]. While RMP-induced alpha-particle losses were found to be acceptably low (less than 1%), additional losses of beam ions were predicted to be up to around 16-17%. Since the beams are required to provide a large fraction of the driven current and auxiliary heating in ITER, losses of this magnitude would imply a significant degradation of plasma performance in this particular scenario. One caveat here is that the RMP fields used in the ITER modelling were computed by solving the vacuum Maxwell equations, and thus did not take into account the plasma response to the RMP coil currents; resistive magnetohydrodynamic (MHD) calculations show that resonant harmonics of RMPs (that is to say, Fourier components of the perturbations with poloidal and toroidal mode numbers m and n such that $m/n = q$, the local safety factor) are strongly suppressed in ITER when plasma effects and rotation are taken into account [6]. Nevertheless the results reported in [4, 5] illustrate the importance of understanding the effects of RMPs on fast ion confinement.

In this paper we present experimental evidence of significant fast ion transport and losses in the Mega Amp Spherical Tokamak (MAST) arising directly from the application of RMPs, and preliminary modelling of such losses carried out using F3D-OFMC, an upgraded version of a particle tracking code described originally in [7]. MAST plasmas typically had major and minor radii $R \simeq 0.95\,\mathrm{m}$ (at the magnetic axis), $a \simeq 0.65\,\mathrm{m}$, elongation κ in the range 1.5-2.5, toroidal field $B_0 \simeq 0.65\,\mathrm{T}$ at $R = 0.75\,\mathrm{m}$, and $I_p \simeq 1\,\mathrm{MA}$. The device was equipped with twelve in-vessel ELM mitigation coils below the midplane and six coils above the midplane, making it possible to have RMPs with a maximum toroidal mode number $n = 3$ in up/down symmetric configurations or up to $n = 6$ when applied below the midplane only [8]. The fast ion population arose mainly from the ionization of two deuterium neutral beams, injected tangentially to flux surfaces with $R \simeq 0.7\,\mathrm{m}$, the ions having initial energies of up to about 70 keV. Such ions typically undergo orbital excursions from flux surfaces Δ_b that are a substantial fraction of the MAST plasma minor radius (Δ_b/a can approach unity in some cases - see e.g. figure 2(b) in [23]), and are thus liable to be affected by non-axisymmetric field perturbations in the peripheral regions of the plasma, such as RMPs. This is particularly the case when the plasma is shifted vertically below the geometric midplane of the vacuum vessel to produce a single-null diverted (SND) configuration; since the beam lines are fixed, the beam deposition profile is then broadened, with the result that there is reduced drive of fast particle pressure-driven instabilities such as fishbones and toroidal Alfvén eigenmodes [10]. However in SND plasmas a higher proportion of the beam ions have orbits that pass close to the ELM-mitigation coils, and a higher level of RMP-induced fast ion transport is thus likely to occur.

The primary rationale for the present study is that it extends the existing database of RMP-induced fast ion transport to the relatively low magnetic field regime of spher-

ical tokamaks, in which the primary fast ions (deka-keV deuterons) undergo orbital excursions from flux surfaces that can be a significant fraction of the plasma minor radius. Recent calculations have shown that in some MAST plasmas the non-resonant component of the RMP field can be significantly amplified rather than suppressed by plasma effects [11]. It is important to quantify the effects of RMPs on fast ions in MAST since an understanding of these effects in such a challenging regime would provide more confidence in the modelling of related processes in ITER.

In section 2 we present evidence obtained experimentally and supported using the TRANSP plasma simulation code that additional fast ion transport was caused by RMPs in some MAST discharges, focussing particularly on SND plasmas. F3D-OFMC computations of fast ion losses with and without $n = 6$ RMPs in an SND MAST plasma are reported in section 3, along with a discussion of possible loss mechanisms. Conclusions and a brief discussion of future work required in this area are presented in section 4.

2 Experimental evidence for RMP-induced fast ion transport in MAST

2.1 Diagnostics of fast ion transport due to RMPs in MAST

Unlike other tokamaks in which RMP-induced fast ion losses have been observed, in MAST it was not possible to detect directly particles of the main energetic ion species when they were expelled from the plasma. However MAST was equipped with several other diagnostics which made it possible to study the behaviour of the beam ions. Neutrons produced in DD fusion reactions (mainly beam-thermal reactions) could be detected using a ^{235}U fission chamber and a four-channel neutron camera (NC), the latter providing information on the spatial distribution of the neutron emission [12]. A fast ion Dα (FIDA) spectrometer was used to measure Doppler-shifted light produced by beam ions when they exchanged electrons with beam or thermal deuterium atoms; measurements of FIDA emission along different lines of sight and at different wavelengths have provided information on changes in the fast ion distribution resulting from MHD instabilities, in particular fishbones [13]. Finally, in the most recent MAST campaign a prototype detector was used to measure fluxes of protons and tritons produced in DD fusion reactions; as in the case of the NC, four channels were available, providing spatial information on the fusion reactivity and hence on the beam ions causing most of these reactions [14].

2.2 Choice of plasmas for study

In the present paper we concentrate, for reasons discussed in the previous section, on SND plasmas. We also focus our attention on MAST plasmas with low current, 400 kA, since the fast ion orbit width scales inversely with this parameter and therefore fast ions are more likely to undergo radial excursions to the outboard plasma edge regions (where the RMP amplitudes tend to be highest) when I_p is low. Even if one restricts

the search to 400 kA SND plasmas, identifying unambiguously the effects of RMPs on fast ion confinement is not straightforward in MAST, due to changes in plasma conditions that often occur when RMPs are applied. In addition to the reduction in ELM amplitudes noted in section 1, RMPs can alter the MHD behaviour of MAST plasmas, which in turn can affect fast ion transport. Moreover RMPs often lead to a reduction ("pump-out") in the plasma density. To leading order this does not affect the total neutron flux since the reduction in target ion density, if ambipolar, is exactly offset in a hydrogenic plasma by an increase in the beam ion slowing-down time and hence the steady-state beam ion density. However, as described below, reductions in density tend to shift the beam deposition profile towards the plasma core, further complicating the interpretation of neutron data.

2.3 Fission chamber measurements

The caveats described above notwithstanding, we now present data from a pair of SND, 400kA MAST pulses in which the application of RMPs had a clear effect on the fast ion population. Figure 1 consists of time traces from pulses 30086 (black) and 30090 (red), showing (a) the RMP coil current per turn (there are four turns in each coil), (b) the total neutron flux S_n measured by the fission chamber, (c) thermal Dα emission from the plasma edge region (i.e. not FIDA emission, which is produced mainly in the plasma core), and (d) the rate of change of poloidal magnetic field measured using a Mirnov coil outside the plasma. The RMPs in pulse 30086 had toroidal mode number $n = 3$. It can be seen that the application of the RMPs coincided with a substantial drop in S_n (approaching 50%) that did not occur in the pulse without RMPs, 30090; until this time the neutron fluxes in the two pulses were very similar. Both pulses were in the high confinement ('H-mode') regime from about 0.3s, before the application of RMPs in pulse 30086; this is indicated in figure 1(c) by relatively low steady-state Dα emission, punctuated by short-lived bursts of emission due to ELMs. As was usual in MAST, the application of RMPs caused the ELMs to have somewhat lower amplitudes and to occur more frequently. As noted in section 1, ELMs have been observed to cause fast ion losses in other tokamaks, and it is intended that a systematic study of ELM-induced fast ions losses in MAST will be carried out in the near future. In the present paper we confine ourselves to the observation that a reduction in ELM amplitudes *per se* would be expected to be accompanied by fewer fast ion losses and thus a higher neutron flux, rather than the suppression in S_n apparent in figure 1(b). The inference that this suppression is likely to have been caused by the RMPs is strengthened by figure 1(d), which shows that the application of RMPs in pulse 30086 was accompanied by a reduction in MHD activity; during this phase mode amplitudes were considerably lower in pulse 30086 than in the pulse without RMPs, 30090. In any case no MHD modes of the type normally associated with anomalous fast ion transport in MAST, such as fishbones, saturated internal kink modes, sawteeth and toroidal Alfvén eigenmodes [15], were observed in either pulse during the period in which S_n was suppressed in pulse 30086.

During the RMP phase in pulse 30086, the electron temperature T_e was typically about 10% lower than in 30090 across much of the plasma. Assuming that the electron

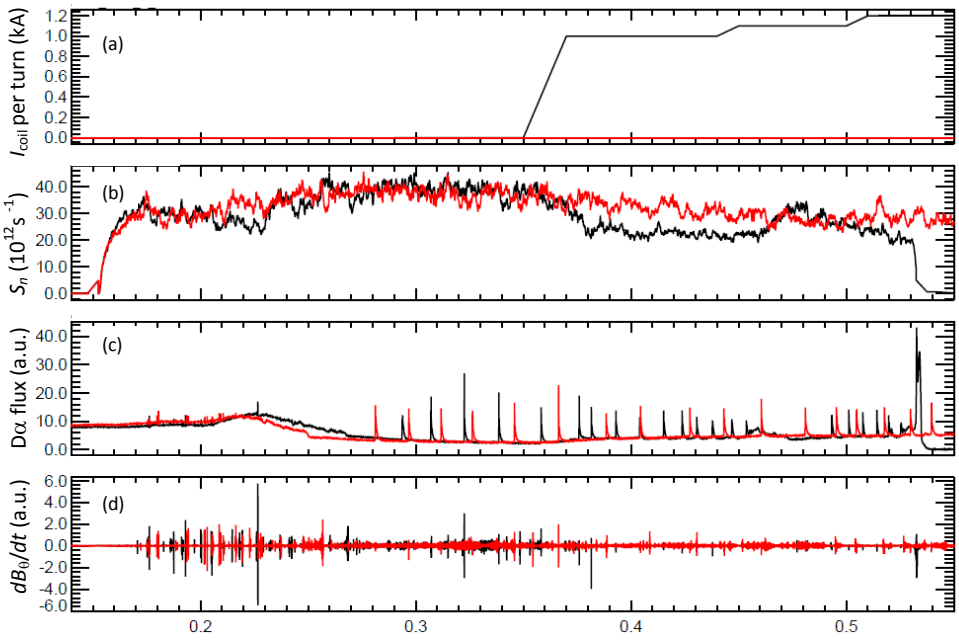

Figure 1: Time traces from MAST pulses 30086 (black) and 30090 (red) showing (a) RMP coil current per turn, (b) total neutron flux, (c) Dα emission, and (d) rate of change of poloidal magnetic field measured using Mirnov coil outside plasma.

heat transport was not significantly affected by the RMPs, some reduction in T_e is to be expected if fast ions were less well-confined, since beam ions provided most of the electron heating. A lower T_e would also account for part of the observed fall in S_n, due to the $T_e^{3/2}$ dependence of the beam ion slowing-down time. Unlike many MAST plasmas with RMPs, the application of field perturbations in pulse 30086 was not accompanied by a strong density pump-out, and so we would not expect the beam deposition profile to have been have significantly affected.

Another point to note in the comparison between these two pulses is that the plasma rotation in pulse 30086 collapsed from around 80 kms^{-1} in the plasma centre to a value close to zero at $t \simeq 0.38$ s, shortly after the RMP coil currents reached their maximum value. RMP-induced braking of the plasma rotation, which was often observed in MAST, tends to increase the neutron emission because the beam ion energy E_b in the rest frame of a thermal deuteron is, on average, higher and the beam-thermal fusion cross-section σ is a strongly increasing function of E_b [16] (MAST plasmas invariably rotated in the direction of beam injection, since the beams were the principal source of momentum input). Comparing the rotation rates in pulses 30086 and 30090, we estimate that the absence of rotation during the application of RMPs in the former implies an increase in σ at the beam injection energy of around 10%. This is further evidence that the subtantial *reduction* of the neutron rate in pulse 30086 is attributable to RMP-induced fast ion transport.

One possibility is that the reduction in neutron rate could have been caused by the

growth of a large amplitude magnetic island as the plasma slowed down. Such "locked modes" were detected in MAST when error fields of sufficiently high amplitude were present [17], and particle simulations have demonstrated that large amplitude islands can greatly enhance fast ion losses in MAST-like plasmas [18]. However locked modes produced distinct signatures in infared camera measurements (splitting of the divertor strike point heat flux) and saddle coil measurements (sudden changes in the sign and amplitude of coil signals), neither of which were detected during the RMP phase in pulse 30086. We conclude that there is no evidence for the reduction of the neutron rate in this pulse being caused by the growth of a locked mode.

In pulse 30086 there was a partial recovery in S_n starting at about 0.46s, coinciding with a temporary transition back to low confinement ('L-mode'). At this time the electron density close to the plasma edge collapsed from a typical H-mode 'pedestal' value of nearly $4 \times 10^{19}\,\mathrm{m}^{-3}$ to a typical L-mode value of about $10^{19}\,\mathrm{m}^{-3}$. The resulting increase in the mean free path of beam neutrals entering the plasma caused the beam deposition profile to be shifted from the plasma edge to the core, resulting in better fast ion confinement; this effect appears to account for most of the observed increase in S_n. The neutron flux started to drop again after a second transition into H-mode at about 0.473s, due apparently to a restored H-mode pedestal shifting the beam deposition profile back towards the plasma edge.

2.4 Fusion proton measurements

Figure 2 shows fluxes of fusion protons recorded in four channels, corresponding to unconfined particle trajectories crossing the midplane at four different major radii (indicated on the figure) for the pulse with RMPs discussed above, 30086. The raw data were binned into 1 ms time intervals; the error bars in figure 2 indicate the Poisson noise associated with the number of counts recorded in each interval. For comparison, the red curves in figure 2 show S_n, normalised to the same scale as the proton rates. Dashed vertical lines indicate the time at which the main RMP coil current ramp-up ended. A similar trend can be seen in all channels and in S_n, but the largest drop in proton rate (more than a factor of two) is apparent in channel 3 whereas the largest absolute rates prior to the application of the RMPs are in channels 1 and 2. This suggests that losses were less likely to occur in regions of the plasma with the highest beam ion density. However the interpretation of these results is not straightforward, due to the fact that fusion protons (unlike neutrons) have curved trajectories. Moreover it should be noted that the beam ion density profiles in SND plasmas such as this are generally hollow, due to the fact that off-axis beam injection was used (see figure 8 in [10]).

2.5 FIDA measurements

Figure 3 shows toroidal FIDA emission versus time in the two pulses discussed above. The left-hand and right-hand plots show data for two different values of R, which here represents the average major radius at which the FIDA line of sight intersects one of the beamlines. The dashed vertical lines indicate the time at which the RMPs were

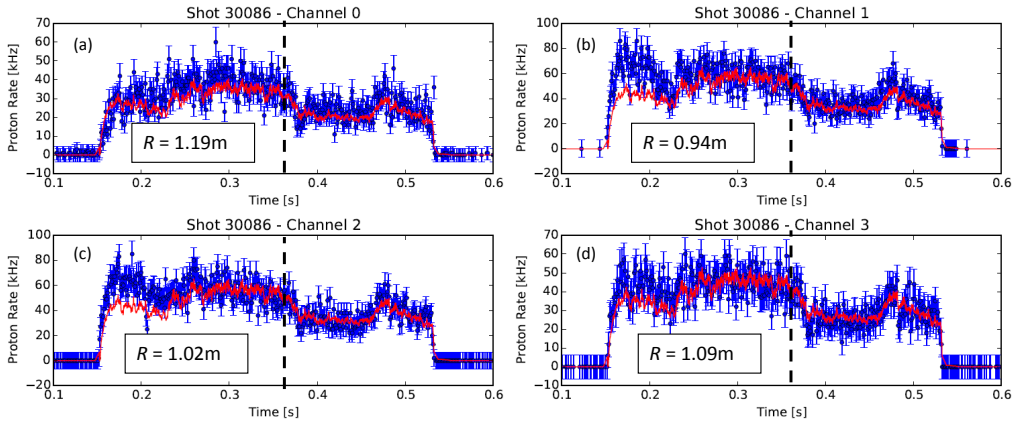

Figure 2: Blue circles with error bars: fluxes of fusion protons recorded in four detector channels during MAST pulse 30086. Red curves: S_n normalised to same scale as proton rates. The dashed lines indicate the time at which the RMP coil current reached its maximum value. The values of R are the average major radii at which protons detected in the foure channels cross the midplane.

first applied. Higher Doppler shifts $\Delta\lambda$ from the Dα rest wavelength $\lambda = 656.3\,\mathrm{nm}$ correspond to higher line-of-sight velocities, hence higher minimum beam ion energies $E_{\mathrm{min}} = m_D c^2 \Delta\lambda^2/(2\lambda^2)$ where $m_D c^2$ is the deuteron rest mass energy. Thus the minumum energies of the fast ions emitting Dα light at the average wavelengths corresponding to the three pairs of plots in figure 3 are 47 keV [(a) and (d)], 52 keV [(b) and (e)] and 58 keV [(c) and (f)]. When the RMPs are applied the emission drops sharply at both values of R and in every wavelength range; there is no obvious dependence on either parameter. The recovery of the fast ion population due to the HL transition at 0.46s is seen in every case, and indeed is more pronounced in FIDA emission than it is in the total neutron rate.

2.6 NUBEAM/TRANSP modelling

The NUBEAM module of the TRANSP plasma simulation code is used to model the collisional evolution of beam ion distributions, with the option of adding *ad hoc* non-collisional transport [19]. The top frame of figure 4 shows the measured total neutron rate in pulse 30086 (black curve) together with synthetic rates computed from NUBEAM simulations with purely collisional transport (green dashed-dotted curve) and with an additional diffusivity $D_a = 1\,\mathrm{m^2 s^{-1}}$ across the plasma and throughout the discharge (blue dotted curve). It can be seen that the synthetic rate obtained from the simulation with anomalous fast ion transport tracks the measured rate fairly well until RMPs are applied, then remains high while the measured rate drops by nearly 50%. Both the simulated rates increase along with the measured rate after the HL transition at about 0.46s, due to the inward shift of the beam deposition profile noted earlier, but the large disparity between simulations and measurements persists until the end of the pulse. In order to achieve near-agreement between measured and simulated neutron

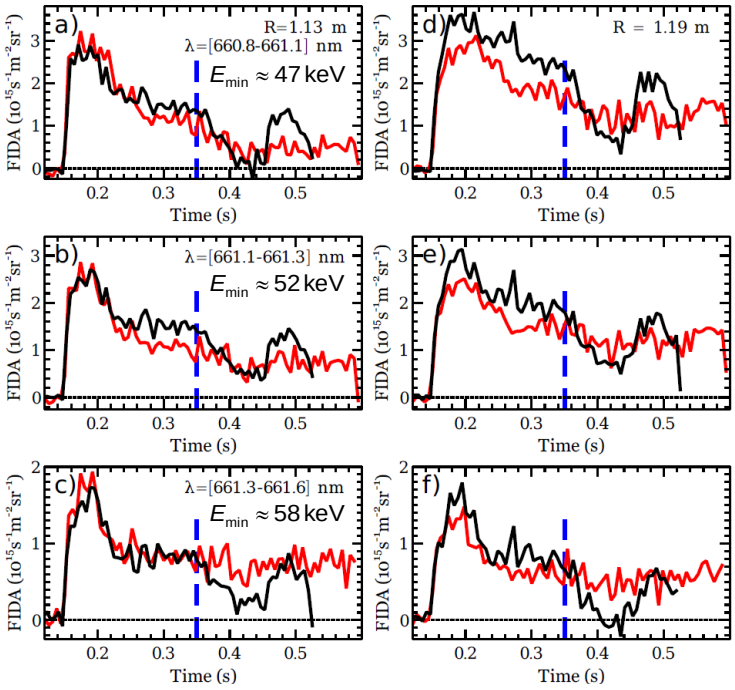

Figure 3: Toroidal FIDA emission versus time in MAST pulses 30086 (black) and 30090 (red) for three wavelength ranges (corresponding to different minimum fast ion energies, indicated on the figure) and two different major radii, R. The blue vertical dashed lines indicate the beginning of the period in which RMPs were applied.

rates, it is normally necessary to set $D_a \neq 0$ (typically a constant value is used) in plasmas with high levels of MHD activity [10]. However shortly after the application of RMPs in 30086, the amplitude of MHD activity dropped considerably (see figure 1(d) and the lower plot in figure 4), which suggests that it would be more appropriate to set $D_a = 0$ in NUBEAM during this phase of the pulse, were it not for the presence of an additional fast ion transport process unrelated to the level of MHD activity. We infer that this additional transport was probably caused by the RMPs.

2.7 Neutron camera measurements

Unfortunately no NC measurements were obtained during pulse 30086. However data were obtained using this diagnostic in other 400kA SND pulses with and without RMPs. Figure 5 shows data from a pair of such pulses, 30276 and 30277. In the second of these pulses the RMP coil current was ramped up very gradually, over a period of 170ms, and then held constant for as long as beam injection was applied, as shown in figure 5(a). The total neutron rates for the two pulses are plotted in figure 5(b), while neutron rates in the three available NC channels are shown in figures 5(c-e). The parameter p indicated in figures 5(c-e) is the tangency major radius of the NC line of sight while Z is the vertical position of the line of sight at the tangency point relative to the midplane of an up-down symmetric plasma. Since these are single null

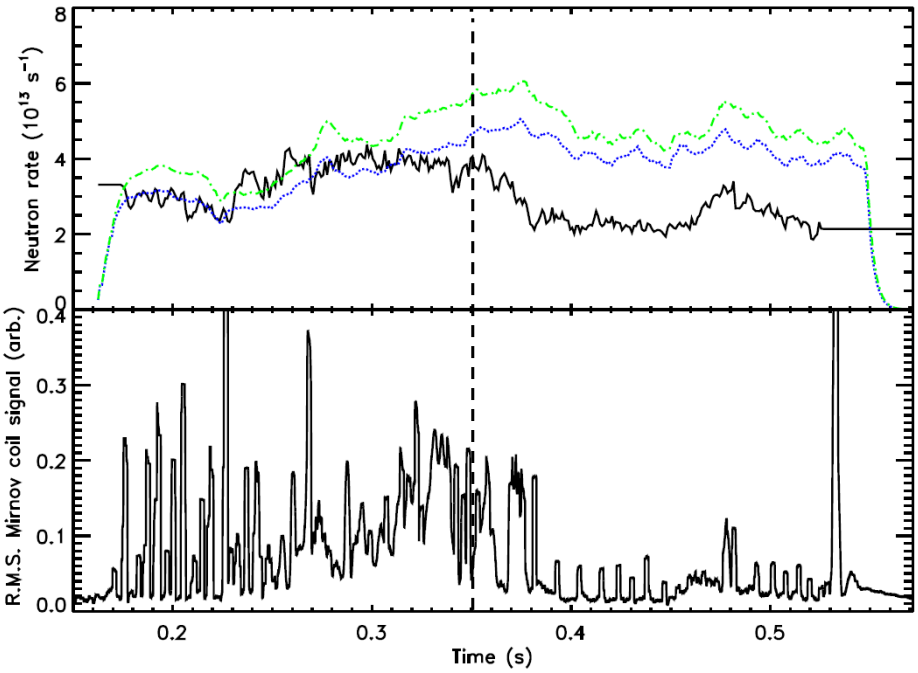

Figure 4: Top plot: total neutron rates measured using the fission chamber (black) and simulated using TRANSP with no anomalous fast ion diffusion (green dashed-dotted curve) and with $D_a = 1\,\mathrm{m^2 s^{-1}}$ (blue dotted curve) in MAST pulse 30086. Bottom plot: root mean square signal measured using an outboard Mirnov coil. The dashed vertical line indicates the time at which the RMPs were first applied.

plasmas, displaced towards the lower divertor, the NC channels with $Z = 0$ had lines of sight that were above the magnetic axis, located at $R \simeq 1\,\mathrm{m}$, $Z \simeq -0.24\,\mathrm{m}$ during the period of RMP application in pulse 30277. Comparing the two pulses, it can be seen that there is a gradual divergence of the total neutron rates and the rates in all NC channels as the coil currents are ramped up, with fewer neutrons being produced in the pulse with RMPs. Out of the three NC channels, the greatest fast ion depletion appears to have occurred in the ones with $p = 0.91\,\mathrm{m}$: between the start of the RMP ramp in pulse 30277 and the end of the pulse, the neutron rates in these two channels fell by nearly a factor of two, whereas the rates in pulse 30276 remained approximately constant or increased slightly in the same period. There was a somewhat smaller (but still significant) relative depletion of the neutron rate in the channel with $p = 1.1\,\mathrm{m}$, $Z = 0$, despite the fact that neutrons in this line of sight were produced by fast ions passing closer to the plasma edge, where more RMP-induced fast ion losses might be expected to occur.

During the period of RMP application, pulse 30277 had smaller ELMs, less MHD activity and a lower toroidal rotation rate than the non-RMP pulse, 30276. As discussed earlier, all of these effects would be expected to cause an increase in the neutron emission rather than the observed suppression. The electron temperature and density profiles were broadly similar, although the temperatures in pulse 30277 were slightly

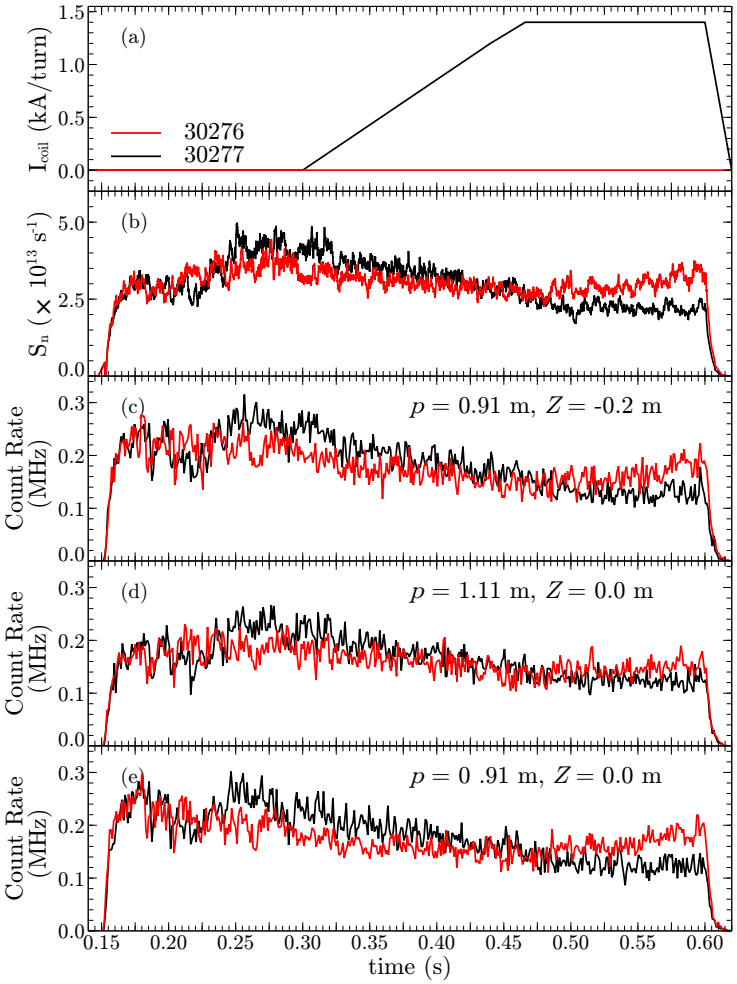

Figure 5: Time traces from MAST pulses 30276 (red) and 30277 (black) showing (a) RMP coil current per turn, (b) total neutron flux, and (c-e) neutron rates in three different NC channels.

lower on average, as expected if there were fewer beam ions available in the plasma to provide auxiliary heating.

We comment finally in this section that some evidence has also been found of fast ion losses due to $n = 6$ RMPs in 600kA SND MAST pulses, but this is generally less clear-cut than in the $n = 3$ 400kA pulses discussed above.

3 Modelling and interpretation

3.1 F3D-OFMC simulations

In addition to the TRANSP simulations with prescribed non-classical fast ion transport described above, first principles-based simulations of beam ions in MAST plasmas with and without RMPs have been carried out using the F3D-OFMC code [7]. Either the

full orbits or the guiding-centre orbits of the beam ions were tracked from birth to thermalization, taking into account collisions with bulk ions and electrons. In the simulations with RMPs, the field perturbations had toroidal mode number $n = 6$ and were calculated in the vacuum approximation using the exact location and geometry of the RMP coils in MAST, the coil current being set equal to the maximum value (5.6kA turns). As discussed in section 1, RMPs in MAST can be significantly amplified by plasma effects. Simulations based on a vacuum model for the field perturbations are thus likely to underestimate fast ion losses. The equilibrium and plasma profiles used in the F3D-OFMC simulations were based on measurements from a single-null MAST pulse, 27205, which had a plasma current of 600kA. For the purpose of modelling collisions, the effective charge state of the plasma $Z_{\rm eff}$ was set equal to 1.5. A particle was considered to be lost when it struck a notional first wall outside the last closed flux surface. Two alternative representations of this were used, designated here as W1 and W2: see figure 6. The actual MAST vacuum vessel lies outside both W1 and W2, at $R \simeq 2\,\mathrm{m}$, but in practice fast ions crossing either of the boundaries shown in figure 6 would almost certainly be lost in a real MAST discharge due to either impact on in-vessel solid surfaces (coils, diagnostics or the centre column) or charge exchange with neutral particles. Both MAST neutral beams were modelled in the simulations, with primary birth energies E_b set equal to 65keV and 51keV. The total beam power was assumed to be 5 MW and, for each beam, ions born at E_b, $E_b/2$ and $E_b/3$ contained, respectively, 74%, 18.5% and 7.5% of the injected power.

A set of six simulations were carried out to determine the effects of the RMPs on the neutral beam power coupled to the plasma, and the sensitivity of the results to the choice of first wall and finite Larmor radius effects. A total of 102,400 particles were tracked in the full orbit simulations with RMPs, and 25,600 particles were tracked in the other simulations. Finite Larmor radius effects were taken into account in the guiding centre simulations for the purposes of calculating the birth profile and particle losses. Table 1 lists the figures obtained in the simulations for the total loss of neutral beam heating power due to fast ion losses; the final column gives the loss of beam power due specifically to RMPs, obtained by subtracting the axisymmetric result for each wall from the total figure. It is evident that the RMP-induced loss of beam heating power found in the simulations is considerable (around 11%) and doesn't depend strongly on either the choice of first wall or finite Larmor radius effects. Full orbit losses are very slightly higher than guiding centre losses, but the differences are very small (comparable to the statistical noise level in the simulations), despite the fact that beam ions are born in MAST with Larmor radii that can be around 10% of the plasma minor radius.

In addition to the overall reduction in beam heating efficiency arising from RMP-induced particle losses, the heat load due to such losses in different regions of the first wall is also an issue of potential concern. Figure 7 shows the toroidally-averaged heat load due to lost ions versus wall number in the W2 full orbit simulation. Using the right hand frame of figure 6 to relate the wall numbers to points in the poloidal cross-section of the MAST vessel, we note that the highest heat loads (up to $0.4\,\mathrm{MWm^{-2}}$) are predicted in this case to occur in the vicinity of the RMP coils. However somewhat different results were obtained in the W1 simulations, and so the computed poloidal distribution of losses depends on the choice of first wall (although the total RMP-

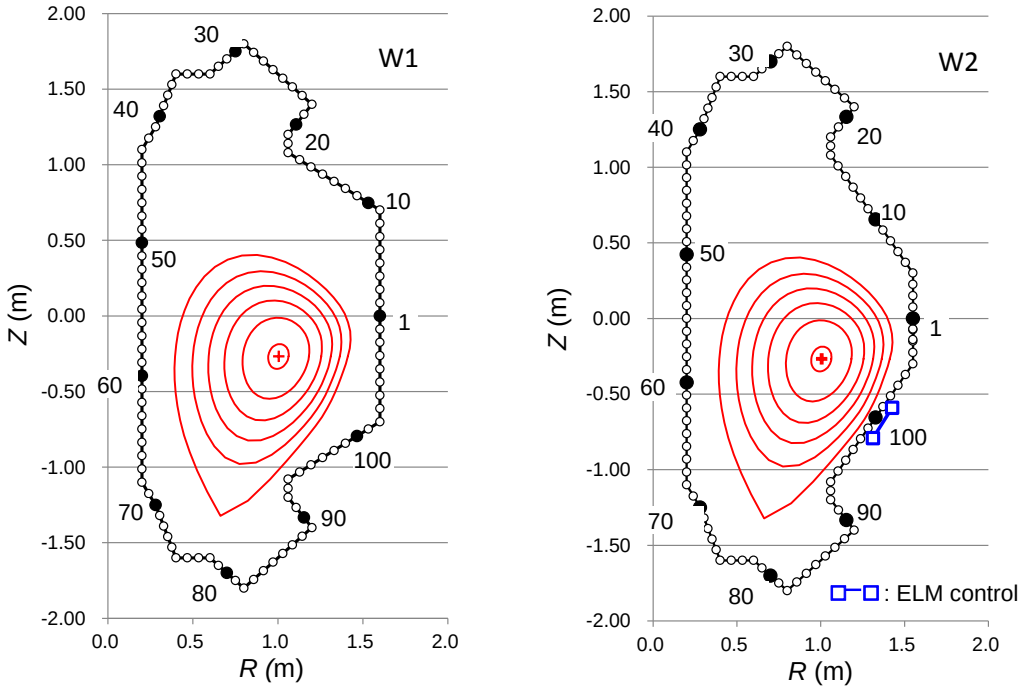

Figure 6: Open circles: representations W1 and W2 of MAST first wall used in F3D-OFMC simulations. The integers next to black circles are "wall numbers" used to characterise the spatial distribution of heat loads due to beam ion losses. Red contours: flux surfaces of MAST equilibrium used in simulations. The equilibrium was obtained using measurements of magnetic fields outside the plasma and of pressure in the plasma periphery in MAST pulse 27205.

induced loss of NBI power does not). When the heat load is plotted as a function of toroidal angle, it is found to have the same periodicity as the RMP coils (i.e. $n = 6$), peaking near the centres of coils producing a radial field perturbation $B_R < 0$ in the plasma. Although MAST was equipped with infrared cameras, which could in principle have detected heating of plasma facing-components arising from fast ion losses, their field of view did not routinely include the ELM mitigation coils, where figure 7 indicates the highest heat loads. No infrared images of the coils are available for shots in which evidence of RMP-induced fast ion transport has been found.

magnetic field	orbit following scheme	wall	total lost power (%)	RMP-induced lost power (%)
axisymmetric	full orbit	W1	5.7	-
$n = 6$ RMPs	full orbit	W1	16.5	10.8
$n = 6$ RMPs	guiding centre	W1	16.2	10.5
axisymmetric	full orbit	W2	11.5	-
$n = 6$ RMPs	full orbit	W2	22.6	11.1
$n = 6$ RMPs	guiding centre	W2	22.1	10.6

Table 1. Neutral beam power losses in F3D-OFMC simulations. The RMP-induced

losses were obtained by subtracting the results for full orbit losses in axisymmetric plasmas from the total figures.

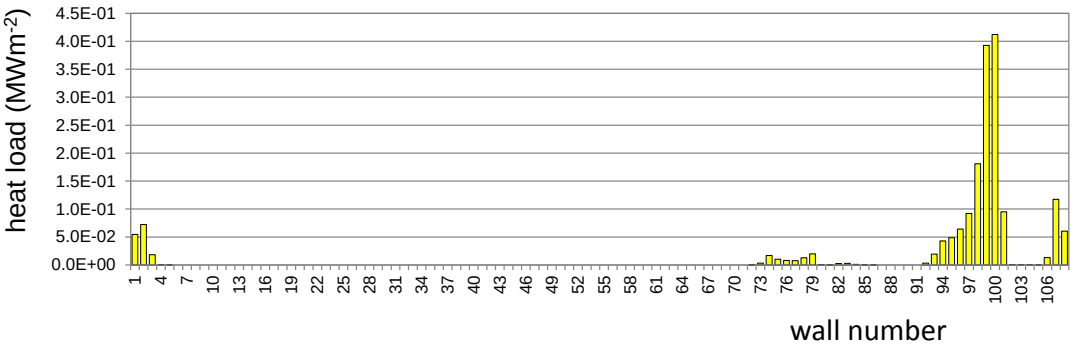

Figure 7: Toroidally-averaged heat load due to lost beam ions versus wall number in F3D-OFMC simulation of MAST SND pulse with $n = 6$ RMPs. Wall representation W2 was used in this case.

Figure 8 shows the loss of neutral beam power normalized to its value after one slowing-down time in the plasma centre (23.6 ms) in one of the simulations with RMPs, (a) over the first 500 μs and (b) over 25 ms. It is apparent that essentially all the losses (a high proportion of which were due to the RMPs) occurred on sub-collisional timescales, before the ions had lost a significant fraction of their initial energy.

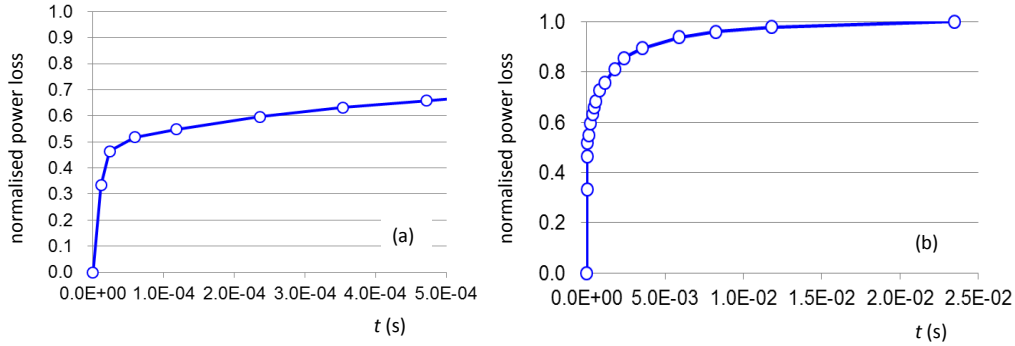

Figure 8: Loss of NBI power (normalised to value after one slowing-down time in plasma centre) due to RMP-induced fast ion transport in F3D-OFMC simulation of MAST SND pulse with $n = 6$ RMPs, (a) over first 0.5ms and (b) over 25ms.

Finally in this subsection, we compare the F3D-OFMC results with simulations of RMP-induced fast ion losses in MAST performed recently using the VENUS-LEVIS guiding centre code [20]. In these simulations a double null-diverted (DND) equilibrium was used, with $I_p = 545$ kA. The effects of RMPs with $n = 3$ were studied, with and without the plasma response to the coil currents taken into account. In the light of the

finding that non-resonant components of RMPs can be amplified rather than suppressed by plasma effects [11], it is interesting to note that higher losses were observed in the VENUS-LEVIS simulations when such effects were included. The absolute losses reported by Pfefferlé and co-workers (see figure 4 in [20]) are somewhat lower than those found using found F3D-OFMC. This is likely to be due mainly to these authors' use of DND plasma equilibria, with fast ion profiles that were relatively core-localised and thus less susceptible to losses caused by field perturbations peaking at the plasma edge. We note also that the toroidal distribution of losses found using VENUS-LEVIS (see figure 3 in [20]) was similar to that observed with F3D-OFMC, i.e. the periodiocity of the losses reflected that of the RMPs causing them.

3.2 Mechanisms of RMP-induced fast ion transport and loss

Pfefferlé and co-workers [20] proposed two possible mechanisms for fast ion loss due to RMPs: transport due to rapid parallel motion in stochastic fields, and particle drifts in three-dimensional fields. To quantify the first of these effects for MAST plasmas, we note that the diffusivity D_s associated with parallel motion in a stochastic field is given by [21]

$$D_s = v_{\|} q R (\tilde{B}/B)^2, \tag{1}$$

where $v_{\|}$ is the parallel component of the fast particle velocity, $\tilde{B}$ is the field perturbation amplitude and B is the equilibrium field. The second of the proposed transport mechanisms can be assessed by noting that the radial grad-B drift speed due to toroidal variation of the field is given by

$$v_r = \frac{n v_{\perp}^2}{R \Omega_i} \frac{\tilde{B} B_{\theta}}{B^2}, \tag{2}$$

where $v_{\perp}$ is the perpendicular component of the fast particle velocity, Ω_i is the fast ion cyclotron frequency and B_{θ} is the poloidal component of the magnetic field. Resistive MHD calculations using the MARS-F code [11] indicate that the total RMP amplitude in MAST $\tilde{B}$ can be of order 10^{-3} T in the plasma core region, where large numbers of fast ions are in well-confined orbits. Setting $B = 0.4$ T, $B_{\theta} = 0.1$ T, $E = 60$ keV and $n = 6$, both of the expressions above suggest that some beam ions could be lost on timescales of less than 1 ms, consistent with the F3D-OFMC results shown in figure 8. However enhanced diffusion due to stochastic fields should expel electrons more readily than fast ions, since the former generally have a higher $v_{\|}$, and so we would expect fast ion losses due to the process described by equation (1) to be accompanied by a strong degradation in electron confinement. This did not occur in the pulses with $n = 3$ RMPs discussed in section 2, suggesting that the three-dimensional drift given by equation (2) is a more likely cause of the fast ion losses. However some caveats are necessary here. It should not be inferred that the n dependence of the drift speed necessarily indicates a monotonic increase of the losses with RMP toroidal mode number, first because the perturbation amplitude $\tilde{B}$ is likely to depend in general on n, and second because the direction of the drift depends on the sign of $\tilde{B}$, which alternates between positive and negative values over a range of toroidal angles equal to $2\pi/n$. In general

the drift would not be expected to average to zero, however, because of finite orbit width, finite Larmor radius and trapped particle effects. An assessment of the overall effects of three-dimensional drifts on fast ion orbits requires a detailed study which is beyond the scope of the present paper.

We comment finally that the RMP-induced fast ion transport could also be determined in part by resonances between the fast particle motion and the RMP perturbation (i.e. wave-particle resonances, with the RMPs playing the role of zero frequency modes).

4 Conclusions and discussion

Measurements of charged and neutral fusion products, together with FIDA measurements and TRANSP modelling, have been shown to contain strong evidence for fast ion transport due to resonant magnetic perturbations (RMPs) with toroidal mode number $n = 3$ in 400kA single-null discharges in the MAST spherical tokamak. In particular the total and spatially-resolved neutron rates dropped by around a factor of two when RMPs were applied, and an even larger drop was observed in one of the channels of a fusion proton detector in one pulse. At the same time there was a reduction in MHD activity. Modelling of this pulse using the TRANSP code reproduces the coarse evolution of the measured total neutron rate until RMPs are applied; after this time, the synthetic neutron rate overestimates the measured rate by around a factor of two, even when non-classical axisymmetric transport is used to evolve the fast ions in TRANSP. We conclude that this shortfall can be attributed to non-axisymmetric effects, specifically RMPs. Simulations using the F3D-OFMC code of a 600kA MAST plasma with n=6 vacuum RMP fields show similar losses for two representations of the MAST first wall, with and without full orbit effects taken into account. In these simulations RMPs were found to cause an 11% loss of neutral beam power.

As discussed in section 2, high levels of RMP-induced fast ion losses are more likely to have occurred in single null MAST plasmas due to the fact that such plasmas had relatively broad fast ion profiles, with some of the fast ions passing close to the coils and hence encountering relatively strong field perturbations. Similar profiles can be achieved in up-down symmetric, DND plasmas if one of the beam lines is displaced vertically from the magnetic axis, as in the upgrade to MAST currently under construction [22]. MAST-Upgrade will also be equipped with ELM mitigation coils: the present work indicates that the effects of RMPs on fast ion confinement should be considered when designing plasma scenarios with off-axis beam injection.

Apart from reducing the efficiency of beam heating and current drive, and increasing heat loads on plasma-facing components, losses of fast ions due to RMPs could also affect plasma rotation. It is well-known that non-ambipolar fast ion losses from a tokamak plasma invariably produce a counter-current torque [23], and hence a toroidal braking of the plasma if it is rotating in the co-current direction, which is normally the case. This provides a possible explanation of the fact that saturated rotation levels in simulations of MAST plasmas with RMPs carried out using the quasi-linear MARS-Q code exceed experimentally-measured values [24].

In this paper we have presented experimental evidence that fast ion confinement in MAST can be significantly degraded by RMPs under certain conditions, and also the results of first principles-based simulations carried out for one particular RMP configuration. Much work remains to be done on the modelling and interpretation of RMP-induced fast ion transport in MAST and MAST-Upgrade, for example to determine the dependence of the losses on RMP toroidal mode number and plasma current. It would be of particular interest to simulate 400 kA SND MAST plasmas with $n = 3$ RMPs, since we have found evidence of high levels of fast particle transport occurring in such plasmas. Experimental studies of this process in MAST-Upgrade would also be highly desirable, particularly in view of the fact that this device, unlike MAST, will be equipped with a fast ion loss detector, which will allow direct measurements of RMP-induced losses to be made.

Acknowledgments

This work has been carried out within the framework of the EUROfusion Consortium and has received funding from the Euratom research and training programme 2014-2018 under grant agreement No 633053 and from the RCUK Energy Programme [grant number EP/I501045]. Helpful discussions with Yueqiang Liu (CCFE), David Pfefferlé (CRPP) and Andrew Thornton (CCFE) are gratefully acknowledged. To obtain further information on the data and models underlying this paper please contact PublicationsManager@ccfe.ac.uk. The views and opinions expressed herein do not necessarily reflect those of the European Commission.

References

[1] Garcia-Munoz M. *et al* 2013 *Plasma Phys. Control. Fusion* **55** 124014

[2] Garcia-Munoz M. *et al* 2013 *Nucl. Fusion* **53** 123008

[3] Van Zeeland M.A. *et al* 2014 *Plasma Phys. Control. Fusion* **56** 015009

[4] Shinohara K. *et al* 2011 *Nucl. Fusion* **51** 063028

[5] Tani K. Shinohara K., Oikawa T., Tsutsui H., Miyamoto S., Kusama Y. and Sugie T. 2012 *Nucl. Fusion* **52** 013012

[6] Liu Y.Q., Kirk A., Gribov Y., Gryaznevich M.P., Hender T.C. and Nardon E. 2011 *Nucl. Fusion* **51** 083002

[7] Tani K., Azumi M., Kishimoto H. and Tamura S. 1981 *J. Phys. Soc. Japan* **50** 1726

[8] Kirk A. *et al* 2010 *Nucl. Fusion* **50** 034008

[9] McClements K.G. and Hole M.J. 2012 *Phys. Plasmas* **19** 072514

[10] Turnyanskiy M., Challis C.D., Akers R.J. Cecconello M., Keeling D.L., Kirk A., Lake R., Pinches S.D., Sangaroon S. and Wodniak I. 2013 *Nucl. Fusion* **53** 053016

[11] Liu Y.Q. *et al* 2012 *Plasma Phys. Control. Fusion* **54** 124013

[12] Cecconello M., Sangaroon S., Turnyanskiy M., Conroy S., Wodniak I., Akers R.J., Ericsson G. and the MAST Team 2012 *Nucl. Fusion* **52** 094015

[13] Jones O.M., Michael C.A., McClements K.G., Conway N.J., Crowley B., Akers R.J., Lake R.J., Pinches S.D. and the MAST team 2013 *Plasma Phys. Control. Fusion* **55** 085009

[14] Perez R.V. *et al* 2014 *Rev. Sci. Instrum.* **85** 11D701

[15] Cecconello M. *et al* 2014 *Plasma Phys. Control. Fusion* **57** 014006

[16] Wesson J.A. 2004 *Tokamaks* 3rd edn (Oxford: Clarendon Press) p5

[17] Howell D.F., Hender T.C. and Cunningham G. 2007 *Nucl. Fusion* **47** 1336

[18] McClements K.G. and Thyagaraja A. 2007 *Plasma Phys. Control. Fusion* **49** 1415

[19] Pankin A., McCune D., Andre R., Bateman G. and Kritz A. 2004 *Comput. Phys. Commun.* **159** 157

[20] Pfefferlé D., Misev C., Cooper W.A. and Graves J.P. 2015 *Nucl. Fusion* **55** 012001

[21] Rechester A.B. and Rosenbluth M.N. 1978 *Phys. Rev. Lett.* **40** 38

[22] Morris A.W. *et al* 2014 *IEEE Trans. Plasma Sci.* **42** 402

[23] McClements K.G. and Thyagaraja A. 2006 *Phys. Plasmas* **13** 042503

[24] Chapman I.T. *et al* 2014 *Nucl. Fusion* **54** 123003